ChemComm

Single-crystal-to-single-crystal guest exchange in columnar assembled brominated triphenylamine *bis*-urea macrocycles

Journal:	*ChemComm*
Manuscript ID	CC-COM-03-2019-001725.R1
Article Type:	Communication

ChemComm

COMMUNICATION

Single-crystal-to-single-crystal guest exchange in columnar assembled brominated triphenylamine *bis*-urea macrocycles

jReceived 00th January 20xx,
Accepted 00th January 20xx

DOI: 10.1039/x0xx00000x

www.rsc.org/

Ammon J. Sindt,[a] Mark D. Smith,[a] Samuel Berens,[b] Sergey Vasenkov,[b] Clifford R. Bowers,[c] and Linda S. Shimizu *[a]

Self-assembly of brominated triphenylamine *bis*-urea macrocycles results in the formation of robust porous materials. Urea hydrogen bonds organize these building blocks into 1-dimensional columns, which pack via halogen-aryl interactions. The crystals are stable when emptied, show defect free channels by ^{129}Xe PFG NMR measurements, and exhibit single-crystal-to-single-crystal guest exchange.

Porous materials are advantageous for catalysis,[1] as nanoreactors,[2] and for the confinement of photo-luminescent compounds[3] as well as for storage,[4] sensing,[5] and separations[6] of small molecules. Key to these processes is how the host and guest influence and interact with each other to afford synergetic properties. Single-crystal-to-single-crystal (SC-SC) transformations can follow these molecular processes by providing atomic details to elucidate the factors that guide the molecular interactions. SC-SC transformations can be triggered under a number of conditions including: temperature,[7] photo-irradiation,[8] guest inclusion,[9] pressure,[10] and mechano-responses.[11] Here, we investigate SC-SC guest exchange in porous organic crystals of triphenylamine *bis*-urea macrocycles.

Typically, hosts for these studies are assembled from rigid materials. Examples include metal organic frameworks (MOFs),[12] hydrogen bonded organic frameworks (HOFs),[13] and porous organic materials.[14] The latter can be beneficial due to the structural versatility organic molecules provide and the ease of forming porous materials simply through crystallization. However, it can be challenging to predict how molecules will assemble in the solid-state. Close-packing principles are often at odds with forming permeable materials. Therefore, molecular families that reliably form porous materials upon crystallization are highly sought after since they offer tunability within their host framework.[15] The Shimizu group employs simple *bis*-urea building blocks that stack into pillars and columns to form nanoporous molecular crystals that can be used as containers for photochemical reactions.[16] While experimental evidence suggests these frameworks remain intact during the process of guest exchange and subsequent photo-reactions, this is our first demonstration of SC-SC transformations. We report a porous organic material made from a triphenylamine (TPA) *bis*-urea macrocycle **1**, which contains two bromo-TPA units (Fig. 1). This macrocycle crystallizes into columnar structures through urea-urea interactions with columns packing together with π-π and halogen-π interactions forming large crystals (35 x 265 μm) that are robust and suitable for SC transformations. Simple heating removes the guest affording homogeneous nanochannels. Immersion of the material into an organic solvent results in a

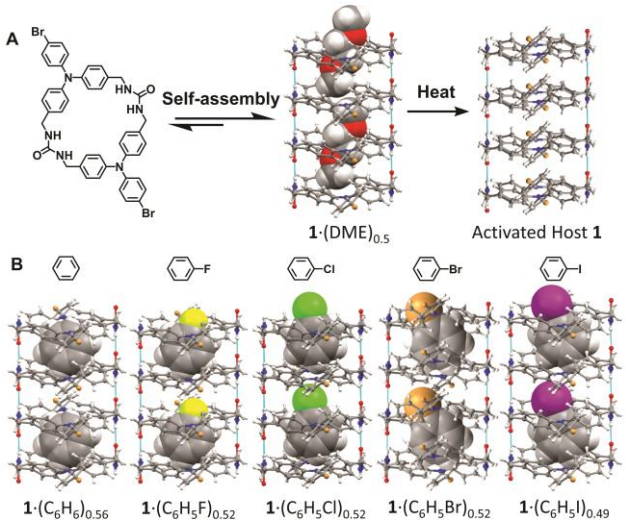

Fig. 1 (A) Self-assembly of macrocycle **1** from the vapour diffusion of DME into DMSO leads to 1D channels. Subsequent heating activates the channels for the loading of different guests. (B) SC-SC transformations observed upon soaking activated host **1** crystals in guest liquids.

[a] *Department of Chemistry and Biochemistry, University of South Carolina, Columbia, SC 29208. Email: SHIMIZLS@mailbox.sc.edu.*
[b] *Department of Chemical Engineering, University of Florida, Gainesville, FL 32611.*
[c] *Department of Chemistry, University of Florida, Gainesville, FL 32611.*
Electronic Supplementary Information (ESI) available: Experimental details and synthesis/characterization of compounds. CCDC 1899526-1899533. For ESI and crystallographic data in CIF or other electronic format see DOI: 10.1039/x0xx00000x

SC-SC transformation to afford a new host:guest complex (Fig. 1B). These complexes organize guests near photoactive TPA units and should consequently enable us to study the effects of closely oriented guests on the optoelectronic properties.

Macrocycle **1** was synthesized by a strategy similar to its linear counterpart.[17] First, commercial bromotriphenylamine was converted to the dialdehyde using a Vilsmeier-Haack reaction followed by hydride reduction resulting in the diol. Once the alcohols were brominated, two TPA units were connected with two triazinanone spacers under basic conditions, resulting in the protected macrocycle. These macrocycles crystallized in chloroform solutions as colourless blocks as a 1:8 macrocycle:$CHCl_3$ solvate, enabling their purification (Fig. S9). Subsequent urea deprotection with diethanolamine under acidic conditions afforded **1** as a beige powder.

Vapour diffusion of 1,2-dimethoxyethane (DME) into a dimethylsulfoxide (DMSO) solution of **1** (~2.5 mg/mL) produced large colourless needles (0.6 x 0.08 x 0.04 mm^3) crystallizing in the space group $P2_1/c$ of the monoclinic system. In this structure, the macrocycle adopts an *anti*-conformation with encapsulated, disordered DME solvent in a 2:1 ratio (Fig. 2A). Both the macrocycle and DME solvent were found on crystallographic inversion centres with the solvent being situated across an additional inversion centre leading to its disorder within the channels. Individual macrocycles assemble into columnar structures organized by the characteristic three-centred urea hydrogen bond, with N(H)···O distances of 2.848(4) and 2.929(4) Å. This creates infinite hydrogen bonded tubes along the crystallographic *b* axis with a macrocycle to macrocycle repeat distance of 4.620(2) Å. π-stacking between neighbouring TPAs provides additional stabilization within the columns (Fig. S17).

Individual columns assemble into pseudo-hexagonal rod-packing arrays, similar to other *bis*-urea structures. However, crystals of **1** are on average ten times larger in width (35 x 265 µm versus 3 x 250 µm, Fig. S10) than any other previously obtained *bis*-urea macrocycle derivative.[16] Hirshfeld analysis was used to identify key interactions that guide assembly and subsequent packing of the columns of **1** to facilitate the growth of larger crystals.[18] Fig. 2B and C shows the d_{norm} surface and highlights the key urea motif driving individual column formation as well as close intercolumnar contacts occurring between the bromine substituents and aryl rings. The halogen-π interactions illustrated in Fig. 2C displays a Br···C_{aryl} distance of 3.303(3) Å, which is shorter the sum of the *vdw* radii (3.5 Å) suggesting that the *p*-bromophenyl groups significantly increases intercolumnar interactions in **1** versus the more cylindrical *bis*-urea macrocycles.[19]

Fig. 3 compares a series of *bis*-urea macrocycles that assembled into similar 1-dimensional columns. Host **1**, phenyl ether (**2**), and benzophenone (**3**) have similar cavity sizes and topographies (Table S3). The cavities are roughly elliptical, displaying cross sectional diameters of ~ 4 Å × 7 Å (Fig. 3A). The walls of these channels are held together by urea hydrogen bonds, with further stabilization coming from aryl stacking interactions. In **2** and **3**, these are edge-to-face π-stacking

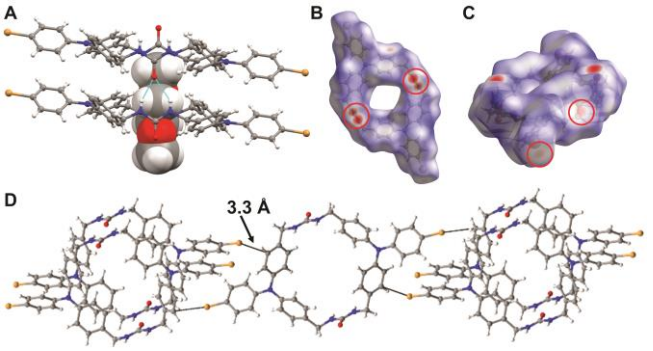

Fig. 2 (A) View along a single column illustrating the 2:1 host:guest ratio and the three-centred urea hydrogen bonding motif. (B) d_{norm} surface showing urea interactions (circled in red). (C) d_{norm} surface showing halogen-π interactions (circled in red). (D) Crystal packing showing select close contacts between columns.

interactions while the extra phenyl groups in **1** lead to offset π stacking. The alternative edge-to-face aryl stacking interactions in **2** and **3** give the channels a curvature highlighted in blue in Fig. 3B, which oscillates back and forth along the length of the columns. These oscillations are also pronounced in the offset-aryl stacked structure of host **1**. The channels of hosts **2** proved to be an ideal substrate for monitoring single file diffusion of Xenon.[20] Therefore, we sought to test if the framework of **1** was stable in the absence of guests to see if it could be used for a similar application.

To monitor guest removal, thermogravimetric analysis (TGA) was applied. Host **1**·DME crystals displayed a one-step desorption curve with a weight loss of 5.3% between 0 and 90° (Fig. S18). Higher temperatures (> 90°C) caused degradation of the material, which was readily detected by NMR. From the percent weight loss, we calculated the macrocycle:guest stoichiometry as 1:0.5. On average a host:guest ratio of 1:0.55 was found over three batches of crystals. The larger crystal size and heavy bromine atoms in **1** facilitated rapid monitoring of the empty host framework by SC-XRD. To ascertain if the host framework would be maintained, one freshly activated crystal

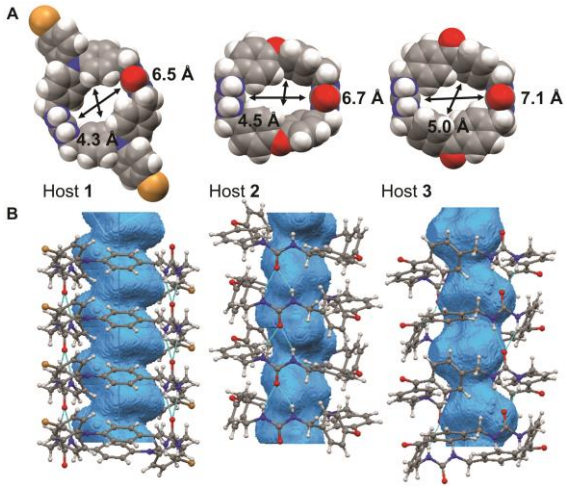

Fig. 3 (A) Pore sizes of different *bis*-urea macrocycles subtracting the *vdw* radii. From left to right the urea spacers are 4-bromotriphenylamine, phenyl ether, and benzophenone. (B) Comparison of their corresponding 1-dimensional columns of **1-3** with their void space highlighted in blue.

was examined immediately after TGA completion and a second crystal after three days on the lab bench in ambient air. Remarkably, the structures, including the columnar framework and packing, were nearly identical to the **1**·DME crystals except that the electron density of the DME was absent (Fig. 1A, activated host). The largest electron density maxima found inside the channels within either data set was 0.21 e^-/ Å^3, i.e. essentially background noise (see S.I.). These results demonstrate the stability of this assembled material under ambient conditions in the absence of guests.

To further characterize the pore space architecture of host **1**, freshly evacuated crystals were pressurized to 9.5 bar (at 298 K) with isotopically enriched Xe gas and sequentially examined by ^{129}Xe NMR. ^{129}Xe NMR has previously been used to study 1D channels[21] since the ^{129}Xe NMR chemical shift tensor is highly sensitive to the pore-space structure and shows dependence on de-shielding due to Xe-Xe interactions, especially at higher Xe loadings in single-file nanotubular pores, where cross-sectional dimensions are comparable to the *vdw* diameter of the Xe atom (0.44 nm).[22,23] Fig. 4A and B show the NMR spectra for ^{129}Xe·**1** at 295 and 243 K referenced to gas phase ^{129}Xe at 0 ppm. A well-defined axially symmetric chemical shift anisotropy (CSA) powder pattern with δ_{iso} = 217 ppm emerges upon cooling the sample to 243 K. This ^{129}Xe CSA tensor is consistent with a high Xe loading in channels with the dimensions of host **1**.[23] The symmetric peak centered near 310 ppm is attributed to highly confined Xe atoms residing in pores with (dynamically averaged) cubic symmetry in host **1**, tentatively identified as the inter-columnar pores (Fig. S20). The ratio of the areas of the adsorbed Xe peaks are close to 3:1 at both temperatures. In the spectrum recorded at 295 K, the small peak that appears near 260 ppm (indicated by the arrow in Fig. 4A) suggests that Xe is in chemical exhange between the two types of pore spaces.

^{129}Xe PFG NMR experiments were performed at 298 K to investigate the diffusion of Xe atoms adsorbed inside the 1-D channels. Unfortunately, short T_2 NMR relaxation times (see S.I.) prevented us from using sufficiently large gradient pulse durations and amplitudes to measure intra-channel diffusion. However, these diffusion studies allowed us to qualitatively examine the exchange of Xe atoms in and out of the channels on the time scale of the diffusion observation (5 - 100 ms). It was found that a complete diffusion attenuation of the gas-phase line could be achieved with an expected gas-phase diffusivity of 6.7x10^{-7} m^2/s at 298 K. However, there was no noticeable diffusion attenuation of the line corresponding to Xe atoms adsorbed in the channels (Fig. 4C). This was seen for all diffusion times used. The observed lack of the diffusion attenuation for the Xe line at 206 ppm allows us to estimate a lower limit of 100 ms on the exchange time (see S.I.). Therefore, we can conclude that there are no defects in the channel walls that might lead such an exchange.

To investigate the ability of this host to absorb and store small molecules, we treated the activated crystals with a series of halogenated benzenes. Host **1**·DME crystals were consistently activated for SC-SC exchange by heating at 90˚C for ~ 2.5 h until no further weight loss was detected via TGA (Fig. S18). Freshly activated crystals (5 mg) were then immersed in a liquid guest (1 mL) for 1 day followed by examination with SC-XRD. SC-SC transformations were observed giving five host **1**·guest structures that displayed 1:0.5 host guest stoichiometry including **1**·C_6H_6, **1**·C_6H_5F, **1**·C_6H_5Cl, **1**·C_6H_5Br, and **1**·C_6H_5I. All the inclusion crystals were found to be isoskeletal with one another, the original DME solvate, and the activated host. Fig. 1B highlights the similarity between these host:guest complexes.

In all cases, the guests showed a moderate amount of disorder within the columns. Fortunately, the halogen-substituted guests permitted more reliable determination despite this disorder due to the larger X-ray scattering factors (especially for Cl, Br and I). The guests aligned in a planar tape-like manner within the channels with guests being crystallographically modelled on two independent sites, one having the halogen-benzene bond more perpendicular to the macrocycle, shown for iodobenzene in Fig. 5A (red structure) with the other in a slightly tilted orientation (Fig. 5A, orange). Both of these sites were located near inversion centres (Fig. 5A, blue and green) giving a total of four possible sites for the guest location, with each having similar occupancies. This disorder was quite similar across all structures. The alignment of the guests in all of these structures may arise from C-H···halogen and/or C-H···π interactions; however, these details are obscured by the crystallographic disorder.

In summary, a brominated TPA *bis*-urea macrocycle assembled to form robust crystals with accessible columnar channels suitable for SC-SC guest exchange. The host is stable when emptied and exhibits confined ^{129}Xe NMR signals when pressurized under Xenon. ^{129}Xe PFG NMR measurements suggest these channels are homogeneous and defect free. Most intriguingly, assembly of this macrocycle orients the individual TPAs close in space to potential guests and enforces close contacts between the two units. Since TPAs are known to undergo chemical or electrochemical oxidation to generate radical cations, these crystalline materials offer potential models for the investigation of electron transfer between organic molecules within confinement. Indeed, linear analogues

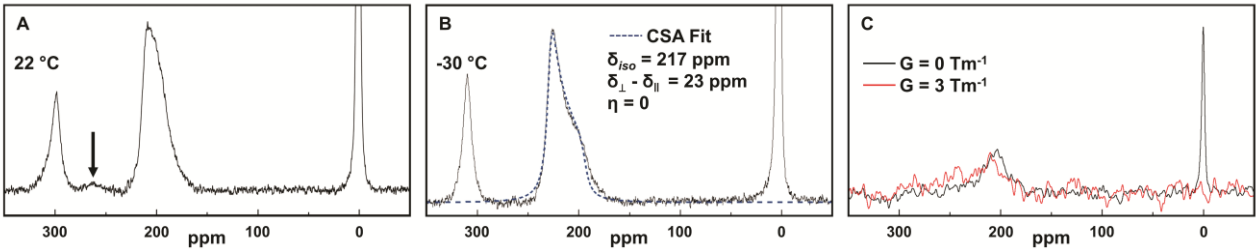

Fig. 4 ^{129}Xe NMR spectra of **1** acquired at 138.45 MHz (11.756 T) at (A) 295 K and (B) 243 K by accumulating 1920 and 960 transients respectively, with a recycle delay of 40x and pulse length of 10 µs. The dashed blue trace is the least-squares fit[24] to an axially symmetric chemical shift anisotropy powder pattern. (C) ^{129}Xe NMR spectra measured using a stimulated echo PFG NMR sequence at 298K and diffusion time 5 ms.

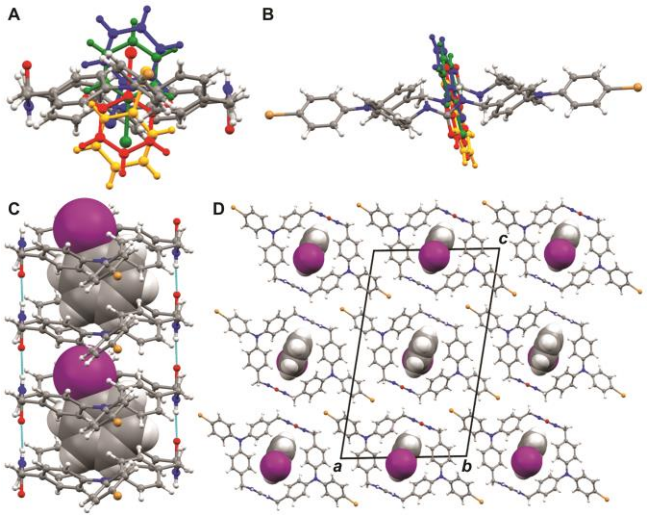

Fig. 5 Crystal views of **1**•C_6H_5I. (A) View of disorder of guest inside the host **1**. Four sites are found. (B) Another view of guest disorder. (C) Space-filled guests inside host **1**. (D) Crystal packing of host **1** with guests. For C and D, disorder was removed for clarity.

of host **1** showed stable and regenerable radical formation upon UV-irradiation in the solid-state.[17] Currently, we are evaluating guests that can undergo electron transfer with the TPA units and hope to report on these in due time.

This work was supported in part by the National Science Foundation (NSF) CHE-1608874 and OIA-1655740. A portion of this work was performed at the National High Magnetic Field Laboratory's AMRIS Facility, which is supported by NSF Cooperative Agreement No. DMR-1644779 and the State of Florida.

Conflicts of interest

There are no conflicts to declare.

References

1 A. Dhakhinamoorthy, M. Alvaro, and H. Garcia, *Chem. Commun.*, 2012, **48**, 11275; S.-Y. Ding, J. Gao, Q. Wang, Y. Zhang, W.-G. Song, C.-Y. Su, and W. Wang, *J. Am. Chem. Soc.*, 2011, **133**, 19816.
2 V. Ramamurthy and J. Sivaguru, *Chem. Rev.*, 2016, **116**, 9914.
3 G. Tabacchi, *ChemPhysChem*, 2018, **19**, 1249.
4 S. Kitagawa, R. Kitaura, and S. Noro, *Angew. Chem. Int. Ed.*, 2004, **43**, 2334; P. Sozzani, S. Bracco, A. Comotti, L. Ferretti, and R. Simonutti, *Angew. Chem. Int. Ed.*, 2005, **44**, 1816; C. M. Kane, A. Banisafar, T. P. Dougherty, L. J. Barbour, and K. T. Holman, *J. Am. Chem. Soc.*, 2016, **138**, 4377.
5 L. E. Kreno, K. Leong, O. K. Farha, M. Allendorf, R. P. Van Duyne, and J. T. Hupp, *Chem. Rev.*, 2012, **112**, 1105; D. J. Wales, J. Grand, V. P. Ting, R. D. Burke, K. J. Edler, C. R. Bowen, S. Mintova, and A. D. Burrows, *Chem. Soc. Rev.*, 2015, **44**, 4290. M. Mastalerz, *Acc. Chem. Res.*, 2018, **51**, 2411.
6 K. Sumida, D. L. Rogow, J. A. Mason, T. M. McDonald, E. D. Bloch, Z. R. Herm, T.-H. Bae, and J. R. Long, *Chem. Rev.*, 2012, **112**, 724; J.-R. Li, J. Sculley, and H.-C. Zhou, *Chem. Rev.*, 2012, **112**, 869; J. Lü and R. Cao, *Angew. Chem. Int. Ed.*, 2016, **55**, 9474.
7 S. Lee, S. Y. Hwang, H. Lee, and O.-S. Jung, *Cryst. Growth Des.*, 2018, **18**, 1278; C.-F. Zhuang, J. Zhang, Q. Wang, Z.-H. Chu, D. Fenske, and C.-Y. Su, *Chem. Eur. J.*, 2009, **15**, 7578.
8 S.-L. Huang, T. S. A. Hor, and G.-X. Jin, *Coord. Chem. Rev.*, 2017, **346**, 112; T. Seki, K. Sakurada, M. Muromoto, and H. Ito, *Chem. Sci.*, 2015, **6**, 1491.
9 V. I. Nikolayenko, D. C. Castell, D. P. van Heerden, and L. J. Barbour, *Angew. Chem. Int. Ed.*, 2018, **57**, 12086; V. I. Nikolayenko, L. M. van Wyk, O. Q. Munro, and L. J. Barbour, *Chem. Commun.*, 2018, **54**, 6975; E. S. O'Brien, M. T. Trinh, R. L. Kann, J. Chen, G. A. Elbaz, A. Masurkar, T. L. Atallah, M. V. Paley, N. Patel, D. W. Paley, I. Kymissis, A. C. Crowther, A. J. Millis, D. R. Reichman, X.-Y. Zhu, and X. Roy, *Nat. Chem.*, 2017, **9**, 1170.
10 B. A. Zakharov, A. S. Marchuk, and E. V. Boldyreva, *CrystEngComm*, 2015, **17**, 8812; B. A. Zakharov and E. V. Boldyreva, *Acta Crystallogr., Sect. B: Struc. Sci., Cryst. Eng. Mater.*, 2013, **B69**, 271.
11 G. Liu, J. Liu, Y. Liu, and X. Tao, *J. Am. Chem. Soc.*, 2014, **136**, 590; M. Jin, T. Sumitani, H. Sato, T. Seki, and H. Ito, *J. Am. Chem. Soc.*, 2018, **140**, 2875.
12 M. Alhamami, H. Doan, and C.-H. Cheng, *Materials*, 2014, **7**, 3198; K. Yan, R. Dubey, T. Arai, Y. Inokuma, and M. Fujita, *J. Am. Chem. Soc.*, 2017, **139**, 11341.
13 H. Wahl, D. A. Haynes, and T. Le Roex, *Cryst. Growth Des.*, 2017, **17**, 4377; Y. Li, M. Handke, Y.-S. Chen, A. G. Shtukenberg, C. T. Hu, and M. D. Ward, *J. Am. Chem. Soc.*, 2018, **140**, 12915.
14 J. T. A. Jones, D. Holden, T. Mitra, T. Hasell, D. J. Adams, K. E. Jelfs, A. Trewin, D. J. Willock, G. M. Day, J. Bacsa, A. Steiner, and A. I. Cooper, *Angew. Chem. Int. Ed.*, 2011, **50**, 749; E. Sanna, E. C. Escudero-Adán, A. Bauzá, P Ballester, A. Frontera, C. Rotger, and A. Costa, *Chem. Sci.*, 2015, **6**, 5466.
15 R. Natarajan, L. Bridgland, A. Sirikulkajorn, J.-H. Lee, M. F. Haddow, G. Magro, B. Ali, S. Narayanan, P. Strickland, J. P. H. Charmant, A. G. Orpen, N. B. McKeown, C. G. Bezzu, and A. P. Davis, *J. Am. Chem. Soc.*, 2013, **135**, 16912.
16 L. S. Shimizu, S. R. Salpage, and A. A. Korous, *Acc. Chem. Res.*, 2014, **47**, 2116.
17 A. J. Sindt, B. A. DeHaven, D. F. McEachern, D. M. M. M. Dissanayake, M. D. Smith, A. K. Vannucci, and L. S. Shimizu, *Chem. Sci.*, 2019, **10**, 2670.
18 F. L. Hirshfeld, *Theor. Chim. Acta*, 1977, **44**, 129; M. A. Spackman and D. Jayatilaka, *CrystEngComm*, 2009, **11**, 19; J. J. McKinnon, D. Jayatilaka, and M. A. Spackman, *Chem. Commun.*, 2007, 3814; S. K. Wolff, D. J. Grimwood, J. J. McKinnon, M. J. Turner, D. Jayatilaka, and M. A. Spackman, *CrystalExplorer (Version 3.1)*, University of Western Australia, 2012.
19 L. S. Shimizu, A. D. Hughes, M. D. Smith, M. J. Davis, B. P. Zhang, H.-C. zur Loye, and K. D. Shimizu, *J. Am. Chem. Soc.*, 2003, **125**, 14972; M. B. Dewal, Y. Xu, J. Yang, F. Mohammed, M. D. Smith, and L. S. Shimizu, *Chem. Commun.*, 2008, 3909.
20 C. R. Bowers, M. Dvoyashkin, S. R. Salpage,C. Akel, H. Bhase, M. F. Geer, and L. S. Shimizu, *ACS Nano*, 2015, **9**, 6343.
21 P. Sozzani, A. Comotti, T. Meersmann, J. W. Logan, and A. Pines, *Angew. Chem. Int. Ed.*, 2000, **39**, 2695; D. V. Soldatov, I. L. Moudrakovski, E. V. Grachev, and J. A. Ripmeester, *J. Am. Chem. Soc.*, 2006, **128**, 6737.
22 J.-L. Bonardet, J. Fraissard, A. Gédéon, M.-A. Springuel-Huet, *Catal. Rev.–Sci. Eng.*, 1999, **41**, 115; C.-Y. Cheng and C. R. Bowers, *ChemPhysChem*, 2007, **8**, 2077.
23 E. Weiland, M.-A. Springuel-Huet, A. Nossov, A. Gédéon, *Microporous Mesoporous Mater.*, 2016, **225**, 41.
24 D. Massiot, F. Fayon, M. Capron, I. King, S. Le Calvé, B. Alonso, J.-O. Durand, B. Bujoli, Z. Gan, and G. Hoatson, *Mag. Res. Chem.,* 2002, **40**, 70.

Crystals of brominated triphenylamine *bis*-urea macrocycles are robust materials with can undergo single-crystal-to-single-crystal guest exchange inside 1-dimensional columns.

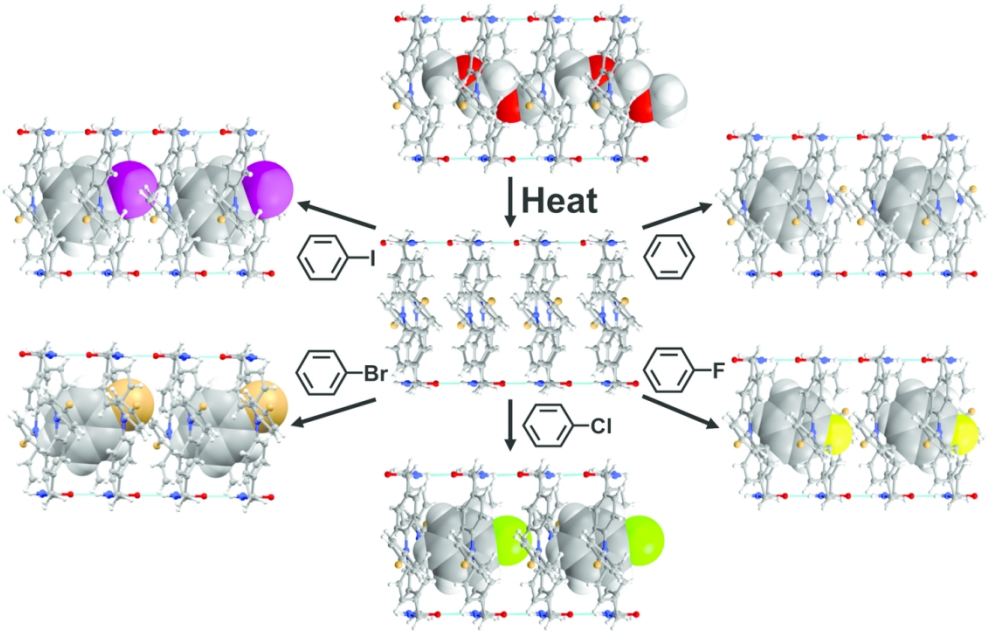

62x40mm (600 x 600 DPI)